Received: 30 November 2018 | Revised: 3 April 2019 | Accepted: 23 April 2019

DOI: 10.1111/ter.12404

PAPER

Terra Nova WILEY

Jurassic igneous rocks of the central Sanandaj–Sirjan zone (Iran) mark a propagating continental rift, not a magmatic arc

Hossein Azizi[1] | Robert J. Stern[2]

[1]Department of Mining, Faculty of Engineering, University of Kurdistan, Sanandaj, Iran

[2]Geosciences Department, University of Texas at Dallas, Richardson, Texas

Correspondence
Hossein Azizi, Department of Mining, Faculty of Engineering, University of Kurdistan, Sanandaj 66177-15177, Iran.
Email: azizi1345@gmail.com
Robert J. Stern, Geosciences Department, University of Texas at Dallas, 800 W Campbell Ave. Richardson, TX 75080.
Email: rjstern@utdallas.edu

Abstract

Jurassic igneous bodies of the Sanandaj–Sirjan zone (SaSZ) in SW Iran are generally considered as a magmatic arc but critical evaluation of modern geochronology, geochemistry and radiogenic isotopes challenges this conclusion. There is no evidence for sustained igneous activity along the ~1,200 km long SaSZ, as expected for a convergent plate margin; instead activity was brief at most sites and propagated NW at ~20 mm/a. Jurassic igneous rocks define a bimodal suite of gabbro-diorite and granite. Chemical and isotopic compositions of mafic rocks indicate subcontinental lithospheric mantle sources that mostly lacked subduction-related modifications. The arc-like features of S-type granites reflect massive involvement of Cadomian crust and younger sediments to generate felsic melts in response to mafic intrusions. We conclude that Jurassic SaSZ igneous activity occurred in a continental rift, not an arc. SaSZ igneous rocks do not indicate that subduction along the SW margin of Eurasia began in Jurassic time.

1 | INTRODUCTION

Understanding the Mesozoic and younger geological evolution of Iran is key for understanding the Alpine-Himalayan orogenic belt because it captures the transition from normal subduction to advanced continental collision like that now occurring between India and Tibet. The Sanandaj–Sirjan Zone (SaSZ) is a key part of the Iran convergent margin and is situated between Cadomian (500–600 Ma) crust of the Iranian plateau and off-scraped sediments of the Zagros fold-and-thrust belt. The SaSZ also bisects the Late Cretaceous Zagros ophiolites into inner and outer belts (Shafaii Moghadam & Stern, 2015). Correct interpretation of Jurassic igneous rocks in the SaSZ is essential for reconstructing the early evolution of the Iranian convergent margin and motivates our study.

Most studies of Jurassic SaSZ igneous rocks consider that these formed at a convergent plate margin (Berberian & Berberian, 1981; Deevsalar et al., 2017; Esna-Ashari, Tiepolo, Valizadeh, Hassanzadeh, & Sepahi, 2012; Khalaji, Esmaeily, Valizadeh, & Rahimpour-Bonab, 2007; Maanijou, Aliani, Miri, & Lentz, 2013; Sepahi, Salami, Lentz, McFarlane, & Maanijou, 2018; Shahbazi et al., 2010). Recent works have increasingly questioned this interpretation (Azizi, Lucci, Stern, Hasannejad, & Asahara, 2018b; Hunziker, Burg, Bouilhol, & Quadt, 2015; Zhang, Chen, Yang, Hou, & Aghazadeh, 2018). In this paper, we compiled published data for SaSZ Jurassic igneous rocks, including 70 U–Pb zircon ages and 1 Rb–Sr whole-rock ages, 170 whole-rock geochemical analyses and 97 Sr–Nd isotope ratios and used these to infer magma sources and tectonic setting. The compilation reveals that these igneous rocks are commonly contaminated by continental crust and show an age progression from SE to NW from 177 to 144 Ma that is best explained by a propagating continental rift on the SW margin of Eurasia.

2 | GEOLOGY OF THE SANANDAJ–SIRJAN ZONE

The SaSZ is a distinctive 50–150 km wide, 1,200 km long terrane that trends SE–NW across SW Iran (Figure 1a). It can be subdivided into three subzones from north to south (Figure 1b). The northern SaSZ consists of Cadomian (500–600 Ma) igneous and metamorphic rocks

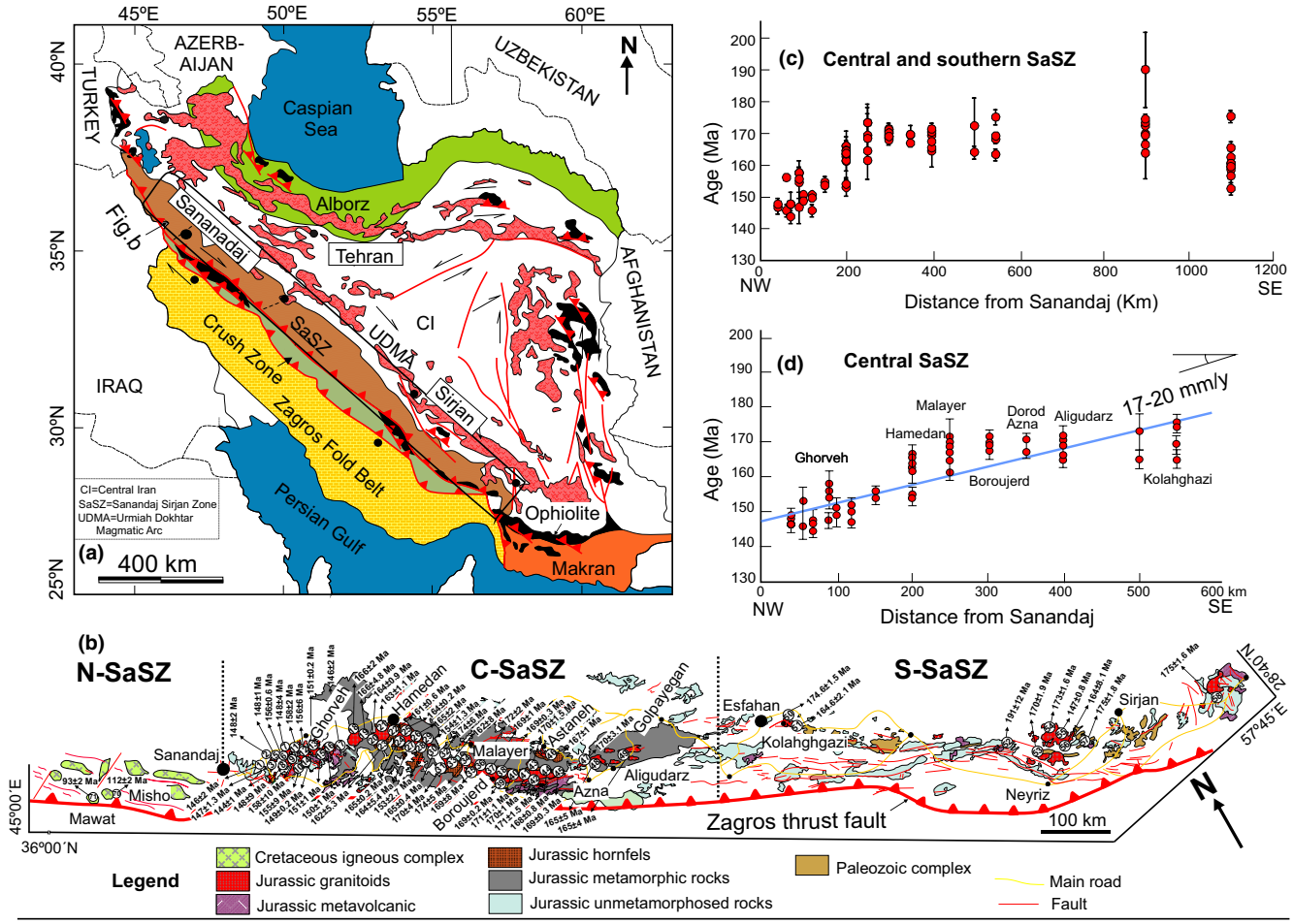

FIGURE 1 (a) Simplified geology map of Iran (Stocklin, 1968) showing the location of the Sanandaj–Sirjan Zone (SaSZ). (b) SaSZ with Precambrian basement and granitoid bodies which are concentrated in the C-SaSZ. Number is location as listed in Table DR1. (c) Age-distance diagram for Jurassic intrusions in the entire SaSZ and (d) only C-SaSZ from Sanandaj city to the south showing the ages of intrusive bodies increasing southeastward [Colour figure can be viewed at wileyonlinelibrary.com]

and Palaeozoic granite (Azizi, Kazemi, & Asahara, 2017) along with mafic to intermediate Cretaceous volcanic rocks (Azizi & Jahangiri, 2008) interbedded with Mesozoic shale, limestone and sandstone. This assemblage was cut by Late Cretaceous granites (Abdulzahra, Hadi, Asahara, Azizi, & Yamamoto, 2018) and Palaeogene granites and volcanics (Azizi et al., 2018b; Azizi et al., 2019; Mazhari et al., 2009).

The central SaSZ (C-SaSZ) is dominated by three lithologies: (a) Cadomian basement, mainly deformed amphibolites and meta-granites (Badr et al., 2018); (b) Regional high-temperature meta-morphic rocks of Early to Mid-Jurassic age (Baharifar, Moinevaziri, Bellon, & Piqué, 2004), with protoliths interpreted as subma-rine MORB and OIB-like volcanics (Azizi et al., 2018b, in press; Tavakoli et al., 2019); and (3c) Jurassic gabbro to granite intrusions (Figure 1b). C-SaSZ felsic intrusions encompass all granite types, especially I-, and S-types along with minor A-types as well as hy-brids of these groups. Pre-existing rocks were heated by Jurassic intrusions and have metamorphic aureoles ranging from a few hundred meters to a few kilometers wide. Al-rich minerals such as garnet, muscovite and aluminosilicates are observed around most intrusions and migmatization is common (Nouri, in press; Sepahi, Jafari, & Mani-Kashani, 2009; Sepahi, in press), consistent with generation of S-type granites by partial melting of metasediments. Granites contain abundant mafic enclaves such as gabbro and diorite and abundant schlieren, suggesting an important role for magma mixing (Figure 2a–f).

The southern SaSZ basement is mainly Palaeozoic metamorphic rocks overlain by unmetamorphosed Triassic and Jurassic sediments (Sheikoleslami, 2015). Early and Middle Jurassic igneous rocks in-cluding calc-alkaline granites have been interpreted as related to Neotethys subduction (Fazlnia, Moradian, Rezaei, Moazzen, & Alipour, 2007; Fazlnia, Schenk, Straaten, & Mirmohammadi, 2009; 2013; Arvin et al., 2007). In contrast, Hunziker et al. (2015) sug-gested a continental rift setting for the 170–175 Ma Jaz Murian dio-rite-trondhjemite-plagiogranite complex.

3 | RESULTS

C-SaSZ Jurassic intrusions include more than 20 big (>8 km across) plutons and many smaller ones (Figure 1b). Most granites have been

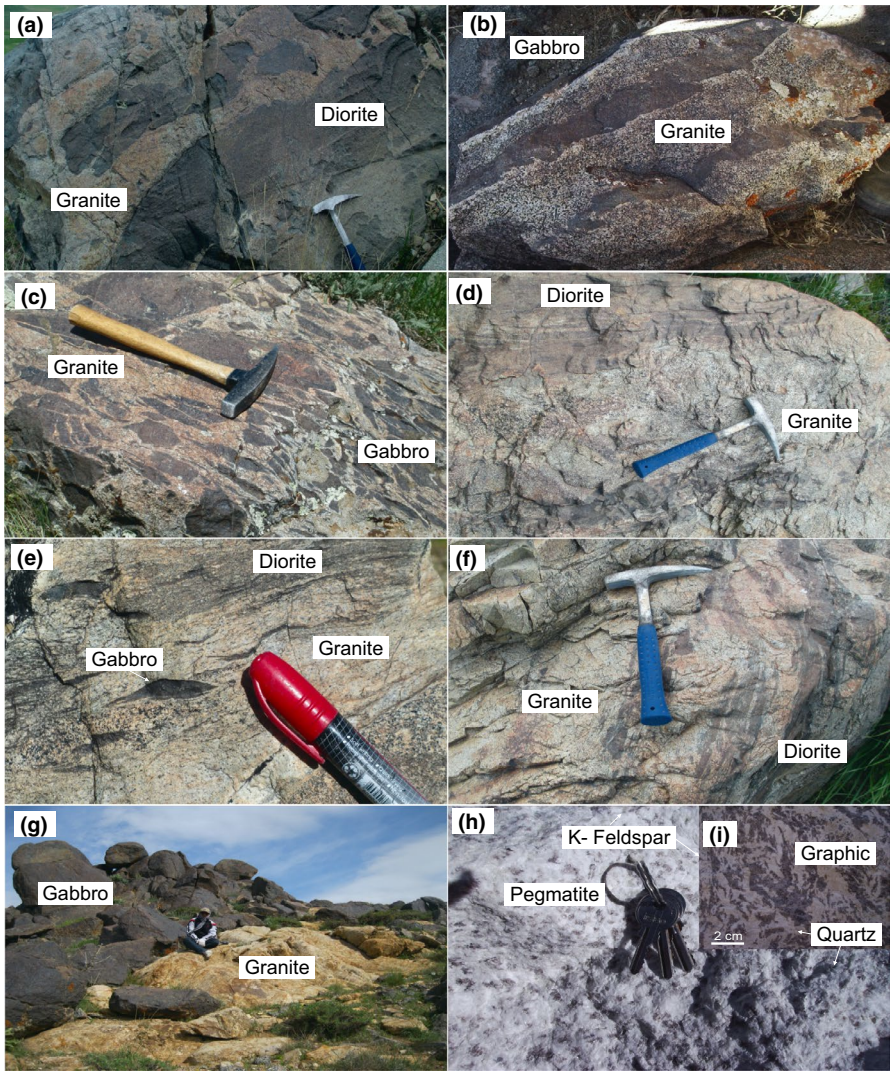

FIGURE 2 Field observations of gabbro-diorite and granite bodies in the central part of the C-SaSZ. (a-f) Dioritic rocks are observed as layers, enclaves and as foliated with schliern in the granites, showing magma mixing between the two magmas. (g) Injection of a pegmatite dike into the diorite. (h) Pegmatite dikes show coarse-grained texture and intergrown K-feldspars and quartz (i) [Colour figure can be viewed at wileyonlinelibrary.com]

dated by zircon U–Pb methods as listed in Table DR1 (Ahadnejad, Valizadeh, Deevsalar, & Rezaei-Kahkhaei, 2011; Azizi, Asahara, Mehrabi, & Chung, 2011; Azizi, Hadi, Asahara, & Mohammad, 2013; Azizi, Najari, et al., 2015; Bayati, Esmaeily, Maghdour-Mashhour, Li, & Stern, 2017; Chiu et al., 2013; Deevsalar et al., 2017; Esna-Ashari et al., 2012; Fazlnia et al., 2007, 2013; Hunziker et al., 2015; Khalaji et al., 2007; Mahmoudi, Corfu, Masoudi, Mehrabi, & Mohajjel, 2011; Mousivand et al., 2011; Shahbazi et al., 2010; Shakerardakani et al., 2015; Yajam et al., 2015; Zhang et al., 2018). The oldest is the 177 Ma Kolah Ghazi intrusion (Bayati et al., 2017) and the youngest are 144 Ma granites near Sanandaj (Azizi et al., 2011; Yajam et al., 2015; Zhang et al., 2018). Plotting granite ages versus distance along the C-SaSZ (Figure 1c) shows younging to the northwest, indicating an age progression of 17–20 mm/a (Figure 1d).

We compiled all chemical data for C-SaSZ intrusions published in international journals over the past few years (Azizi & Asahara, 2013; Azizi et al., 2011; Azizi, Najari, et al., 2015; Deevsalar et al., 2017; Esna-Ashari et al., 2012; Khalaji et al., 2007; Maanijou et al., 2013; Mahmoudi et al., 2011; Shahbazi et al., 2010); these data are summarized in Table DR2. We do not use Ta because several of these studies pulverized in tungsten carbide. A total alkalis versus SiO_2 plot shows that most analyses plot in the sub-alkaline field (Middlemost, 1985) (Figure 3a). Plotting these samples on diagrams designed to reveal tectonic setting gives equivocal results. Mafic rocks scatter on the Ti–V variation diagram (Shervais, 1982), from arc to alkaline (Figure 3b). Most granitic rocks plot in the peraluminous field in the Shand (1943) diagram (Figure 3c). Based on their high Nb and low Y contents, C-SaSZ granites mostly plot in the post-orogenic field in the Pearce, Harris, and Tindle (1984) diagram (Figure 3d).

Because of the likelihood that granitic magmas reflect strong crustal inputs, we focused on mafic (<52 wt.% SiO_2) samples, which should be less contaminated. Some mafic rocks are enriched in large ion lithophile elements (LILEs) and light rare-earth elements (LREE). Minor negative Nb anomalies are observed, but not the deep anomalies expected for arc magmas. Mafic rocks show low K_2O contents and generally plot outside of the arc field. On the Nb–Nb/U diagram (Pearce, 2008) most SaSZ samples plot outside the arc field (Figure 4a). In the Nb/Yb–Th/Yb diagram (Figure 4b; Pearce, 2008) they fall mostly in the field of arc rocks but this is also where mafic magmas contaminated by continental crust plot. Based on the

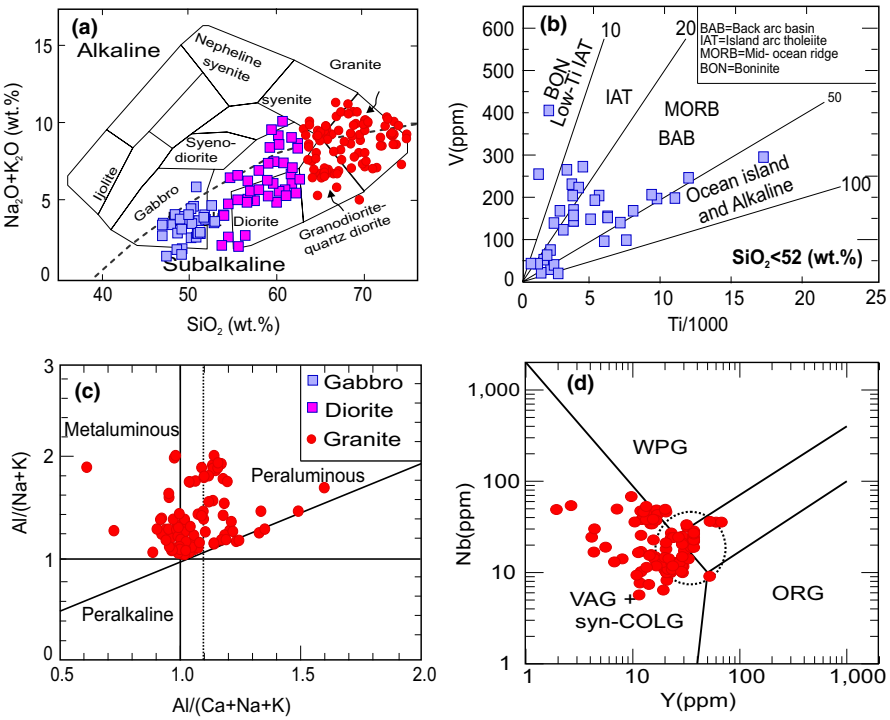

FIGURE 3 Chemical composition of C-SaSZ mafic (blue squares), intermediate (magenta squares) and felsic (red dots) intrusions (Azizi & Asahara, 2013; Azizi et al., 2011; Azizi, Najari, et al., 2015; Deevsalar et al., 2017; Esna-Ashari et al., 2012; Khalaji et al., 2007; Maanijou et al., 2013; Mahmoudi et al., 2011; Shahbazi et al., 2010). (a) Total alkalies versus SiO_2 (Middlemost, 1985), showing wide variations from gabbro to granite. (b) Mafic rocks show unusual scatter on the Ti-V variation diagram (Shervais, 1982), plotting in all fields, from island arc tholeiite to alkaline. (c) Granitic rocks plot in both metaluminous and peraluminous fields (Shand, 1943). (d) Granitic rocks show affinities with post-orogenic granite (dotted field) on the Nb-Y discriminant granite tectonic setting diagram (Pearce et al., 1984). ORG = Ocean ridge granite, WPG = within-plate granite, VAG = volcanic arc granite, syn-COLG = syn-collisional granites [Colour figure can be viewed at wileyonlinelibrary.com]

abundances of high field strength elements Nb, Zr and Y and LILE Th, the samples mainly plot in the plateau basalt field with some affinity to OIB (Condie, 2005; Figure 4c,d). The samples mainly plot in the continental rift field in the La–Nb–Y diagram (Cabbanis & Lecolle, 1989, Figure 4e). Trace elements normalized to primitive mantle (Sun & Macdonough, 1989) sometimes show positive anomalies for some elements such as Th, Pb and K (Figure 5a). The low contents of LILEs such as Rb, Ba and K and positive trend from the LILE to HSFEs observed on these diagrams confirms the role of a depleted source such as subcontinental mantle (Figure 5a,b). The low slope from the LREEs to HREEs does not indicate a highly metasomatized mantle source for the mafic rocks (Figure 5c). In summary, the compositions of C-SaSZ mafic rocks may be confused with arc igneous rocks but careful examination shows that these compositions are better explained as OIB-like magmas contaminated by continental crust.

Initial $^{87}Sr/^{86}Sr$ and $^{143}Nd/^{144}Nd$ for C-SaSZ intrusions (Table DR2; Azizi & Asahara, 2013; Azizi et al., 2011; Azizi, Najari, et al., 2015; Deevsalar et al., 2017; Esna-Ashari et al., 2012; Khalaji et al., 2007; Shahbazi et al., 2010) range widely. Mafic rocks mostly show positive $\varepsilon_{Nd}(t)$ and low $^{87}Sr/^{86}Sr_{(i)}$ and plot in the depleted mantle field (Figure 6a). Granitic rocks show large variations of $\varepsilon_{Nd}(t)$, from +5 to −5 with variable $^{87}Sr/^{86}Sr_{(i)}$, defining a trend that extends towards compositions expected for upper continental crust (Figure 6b). Nd model ages (Jahn, Wu, Lo, & Tsai, 1999) suggest that mafic magmas were generated from young depleted mantle and perhaps subcontinental lithosphere, whereas granitic magmas had larger contributions from Cadomian continental crust and sediments (Figure 6a,b).

4 | DISCUSSION

Studies of SaSZ igneous rocks can be usefully subdivided into those carried out before and after 2007. A major weakness in early studies was the lack of U–Pb zircon ages for Jurassic igneous rocks. Interpretations were based on the observation that SaSZ intrusions cut the Jurassic metamorphic complex, suggesting that these were Cretaceous intrusions (Berberian & Berberian, 1981). Some Rb-Sr and K-Ar ages for Hamadan granites (81–64 Ma; Valizadeh & Cantagrel, 1975) and Astaneh granite (120–70 Ma; Masoudi, Yardley, & Cliff, 2002) supported this age assignment. These ages allowed these intrusions to be linked with Late Cretaceous Zagros ophiolites and encouraged the interpretation that both were related to Cretaceous convergent margin and collision processes. After 2007, U–Pb zircon dating showed that SaSZ igneous rocks were 190–140 Ma and unrelated to the ophiolites. This created a new problem: how to connect these granites to convergent margin processes? Attempted solutions

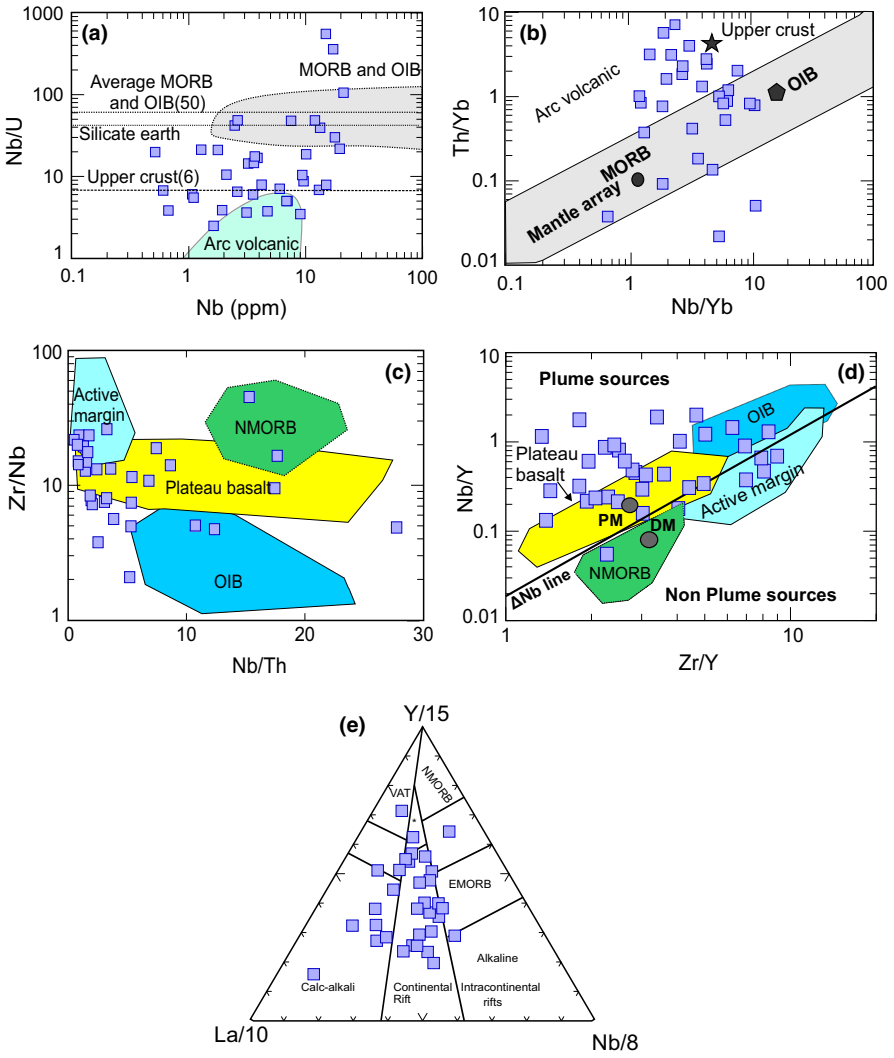

FIGURE 4 Plots of mafic samples (<52 wt.% SiO_2) on diagrams designed to reveal tectonic affinity. (a) In the Nb/U-Nb variation diagram (Pearce, 2008) most samples plot outside the arc field. (b) In the Nb/Yb-Th/Yb diagram (Pearce, 2008) samples show mixing between the mantle and upper crustal components. (c) Zr/Nb versus Nb/Th diagram shows mostly low ratios of Nb/Th in C-SaSZ mafic rocks, with many samples showing affinities to plateau basalts (Condie, 2005). (d) Nb/Y versus Zr/Y diagram (Condie, 2005) show that SaSZ samples are similar to plateau basalt and OIB. (e) in the La/10-Y/15-Nb/8 (Cabbanis & Lecolle, 1989) diagram, most samples plot in the field for continental rifts. Fields for MORB/OIB and arc volcanism are from Chang et al. (2001), upper continental crust composition after Rudnick and Gao (2004) [Colour figure can be viewed at wileyonlinelibrary.com]

led to many new suggestions for SaSZ Jurassic granites, for example slab window, arc-continent collision, slab roll-back, slow subduction, low angle and oblique subduction and various ages of subduction and collision including Triassic, Jurassic and Cretaceous. Now, the many new zircon U–Pb ages for these intrusions has established the Jurassic age of these intrusions. We also have much better chemical and isotopic data for these rocks.

Systematic interpretation of Jurassic SaSZ igneous rocks lags behind the improved dataset. These are still generally regarded as having formed in a magmatic arc due to subduction of Neotethys beneath Iran (e.g. Ahadnejad et al., 2011; Deevsalar et al., 2017; Esna-Ashari et al., 2012; Khalaji et al., 2007; Sepahi, 2008). Our compilation provides no support for this hypothesis and shows that the weak arc-like chemical features are better explained by massive contamination of mafic magmas by continental crust and sediment.

Our review of whole-rock compositions, Sr–Nd isotope ratios and radiometric ages for SaSZ Jurassic igneous bodies reveals their remarkable variety. The most important observation is that Jurassic C-SaSZ bodies show a clear age progression, from 177 Ma in the SE to 144 Ma in the NW (although sparse data in the S-SaSZ suggest a SE-ward age progression; Figure 1c). Such a progression is unexpected for arc magmatic activity, which should be contemporaneous all along the arc and should persist for tens of millions of years. The inferred migration rate of 17–20 mm for C-SaSZ Jurassic intrusions is consistent with SE motion of Iran over a fixed hotspot, a slowly moving hotspot beneath a fixed plate, or both. Because there is no evidence for such a Eurasian plate vector and the suggestion that igneous activity in the S-SaSZ also propagated to the SE, we prefer to interpret Jurassic SaSZ igneous activity as reflecting formation in a propagating continental rift in Middle to Late Jurassic time (Figure 7).

A propagating rift model is consistent with observed geochemical and isotopic variations for Jurassic SaSZ igneous rocks. C-SaSZ granites formed by mixing mafic magma derived by partial melting of asthenosphere and subcontinental lithospheric mantle—with positive $\varepsilon_{Nd}(t)$ and low $^{87}Sr/^{86}Sr_{(i)}$—with upper continental crust and sediments having negative $\varepsilon_{Nd}(t)$ and high $^{87}Sr/^{86}Sr_{(i)}$. Varying proportions of these two end-members generated the different types of C-SaSZ igneous rocks, with gabbros being less contaminated and granites being more contaminated. Such an interpretation also explains the large volume of tholeiitic mafic bodies, abundance of S-type granite and the existence of some A-type granites (Zhang et al.,

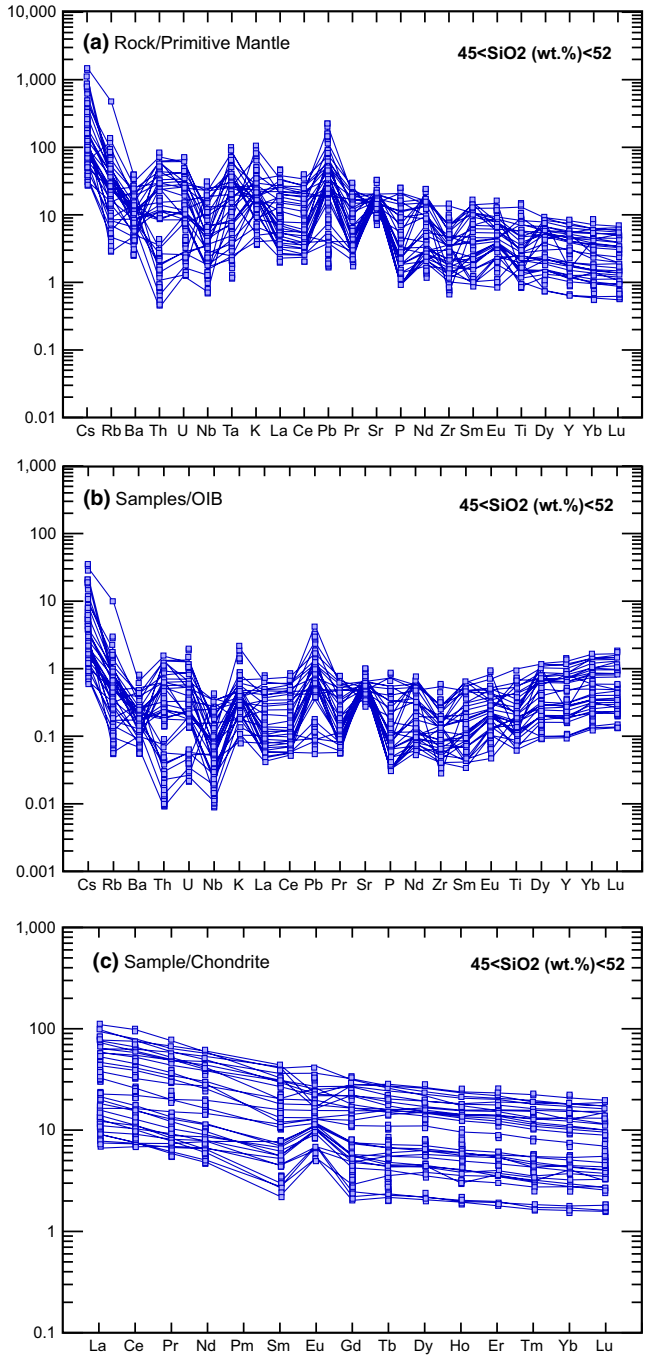

FIGURE 5 Trace element data for C-SaSZ mafic igneous rocks compared to primitive mantle (a), ocean island basalt (OIB) (b) and chondrite (c). Data used for normalization are from Sun and McDonough (1989) [Colour figure can be viewed at wileyonlinelibrary.com]

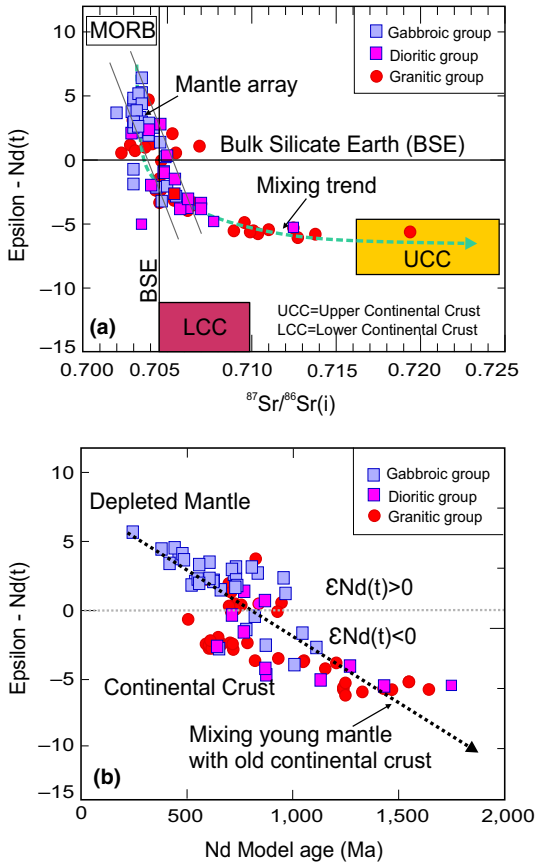

FIGURE 6 Nd-Sr isotopic data for C-SaSZ Jurassic igneous rocks. (a) Most mafic rocks show positive $\varepsilon_{Nd}(t)$ and low $^{87}Sr/^{86}Sr_{(i)}$ and plot in the depleted mantle field, whereas granites show mixing between melts of subcontinental lithospheric mantle and upper continental crust. (b) Nd model ages (Jahn et al., 1999) show that mafic magmas were dominantly generated from young depleted mantle with positive $\varepsilon_{Nd}(t)$ and granitic rocks with negative $\varepsilon_{Nd}(t)$ were mostly derived from older continental crust [Colour figure can be viewed at wileyonlinelibrary.com]

2018). It also explains the absence of arc-type mineralization (such as porphyry deposits) in the SaSZ and the presence of W-Sn mineralization related to S-type granites.

Evidence of rifting also exists farther NW from the C-SaSZ. Recently reported tectonostratigraphy of Jurassic sedimentary rocks in western Iran (Stefano et al., 2018) and magmatic activities in the Khoy area, NW Iran (Lechmann et al., 2018) confirm that Jurassic extension affected the region. SaSZ metabasaltic rocks interbedded with Jurassic metasediments further indicate an extensional basin with OIB-type magma affinity (Azizi et al., 2018b; Nasr-Esfahani, 2012; Tavakoli et al., 2019). In the northern SaSZ northwards of Sanandaj (Figure 1b), ages of igneous rocks young northward for example 112 ± 2 Ma acidic and volcanic rocks (Abulzahra et al., 2018) and also the 93 ± 2 Ma (Rb–Sr mineral isochron) for the Mawat mafic plume complex (Azizi et al., 2013). In the N-SaSZ, the mafic components are much more dominant compared to the C-SaSZ. We do not yet know what if any relationship the N-SaSZ Cretaceous igneous rocks have with Jurassic igneous rocks of the C-SaSZ, but this wide age range is inconsistent with arc magmatism and consistent with continental rifting. The continental rift model for the C-SaSZ can explain the wide age range of Jurassic igneous rocks as manifesting NW propagation of rifting at ~ 20 mm/a (Figure 7a,b), but we still have much to learn about how this tectonic regime was manifested to the NW and SE.

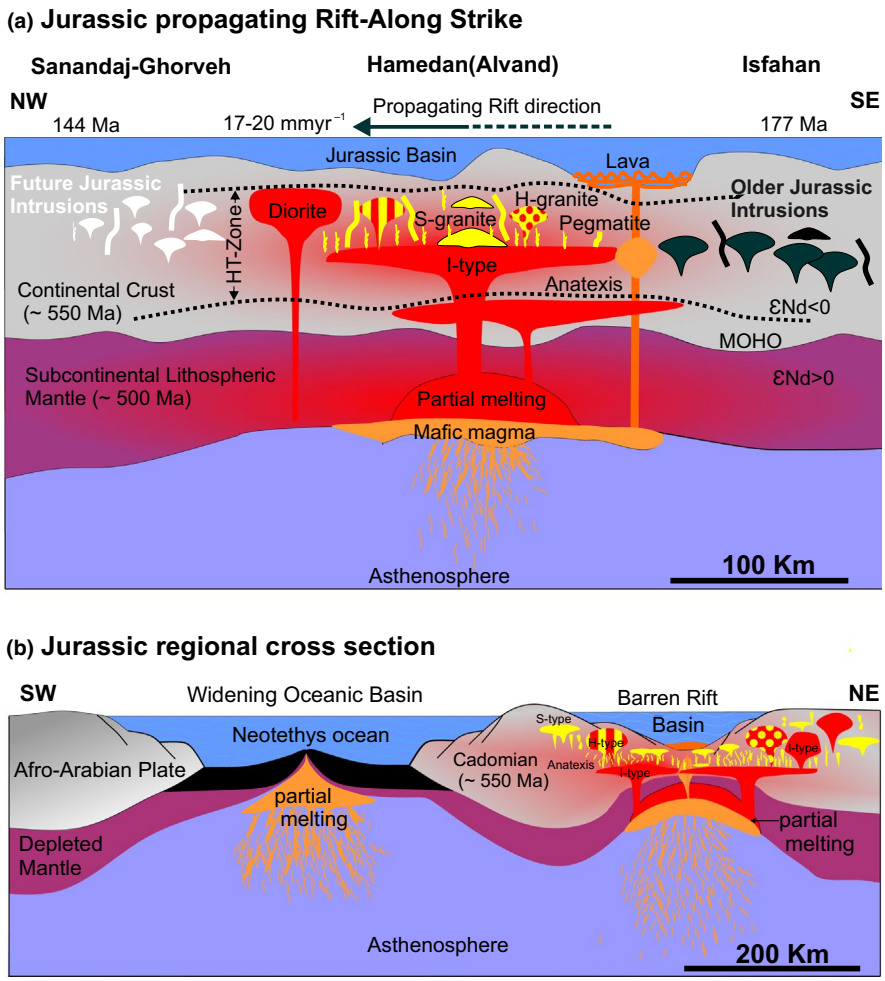

FIGURE 7 Schematic representation of magmatotectonic setting of C-SaSZ in Jurassic time (a) NW-SE profile along the C-SaSZ. This profile shows a continental rift propagating northwestward ~ 20 mm/a in the C-SaSZ and how Jurassic SaSZ igneous bodies were generated. The model shows how different sources for C-SaSZ granitic rocks were involved. The upwelling of hot magma heated subcontinental lithospheric mantle, causing partial melting to generate mafic melts. Injection of mafic magma into the overlying continental crust was responsible for metamorphism, migmatization and partial melting of continental crust to produce S-type granites. (b) SW–NE cross-section nearly perpendicular to the C-SaSZ continental rift. It shows development of a metallogenically barren rift in the SaSZ and also how metamorphism, volcanism and plutonism occurred at the same time that seafloor spreading occurred in Neotethys [Colour figure can be viewed at wileyonlinelibrary.com]

5 | CONCLUSIONS

The tectonic setting of Jurassic igneous activity in the C-SaSZ of Iran must be re-evaluated from a regional perspective, not on the basis of individual intrusions. Such a perspective shows that Jurassic igneous bodies young from SE to NW. This systematic age progression is more consistent with magma genesis associated with a propagating continental rift, not a magmatic arc above a Neotethys subduction zone. The paucity of Jurassic igneous rocks in the N-SaSZ and lower abundance in the S-SaSZ show that the most intense rifting happened in the C-SaSZ. These results require a critical re-examination of Mesozoic tectonic scenarios for SW Eurasia.

ACKNOWLEDGEMENTS

This version benefitted from reviews by Dave Lentz, G. Wörner, two anonymous referees and editor J.P. Morgan. This is University of Texas at Dallas Geosciences contribution number 1320.

ORCID

Hossein Azizi https://orcid.org/0000-0001-5686-4340

Robert J. Stern https://orcid.org/0000-0002-8083-4632

REFERENCES

Abdulzahra, I. K., Hadi, A., Asahara, Y., Azizi, H., & Yamamoto, K. (2018). Petrogenesis and geochronology of Mishao peraluminous I-type granites, Shalair valley area, NE Iraq. *Chemie Der Erde*, *78*, 215–227. https://doi.org/10.1016/j.chemer.2018.01.003

Ahadnejad, V., Valizadeh, M. V., Deevsalar, R., & Rezaei-Kahkhaei, M. (2011). Age and geotectonic position of the Malayer granitoids: Implication for plutonism in the Sanandaj-Sirjan Zone, W Iran. *Neues Jahrbuch Für Geologie Und Paläontologie-Abhandlungen*, *261*, 61–75. https://doi.org/10.1127/0077-7749/2011/0149

Arvin, M., Pan, Y., Dargahi, S., Malekizadeh, A., & Babaei, A. (2007). Petrochemistry of the Siah-Kuh granitoid stock southwest of Kerman, Iran: Implications for initiation of Neotethys subduction. *Journal of Asian Earth Sciences*, *30*, 474–489. https://doi.org/10.1016/j.jseaes.2007.01.001

Azizi, H., & Asahara, Y. (2013). Juvenile granite in the Sanandaj-Sirjan Zone, NW Iran: Late Jurassic-Early Cretaceous arc–continent collision. *International Geology Review*, *55*, 1523–1540. https://doi.org/10.1080/00206814.2013.782959

Azizi, H., Asahara, Y., Mehrabi, B., & Chung, S. L. (2011). Geochronological and geochemical constraints on the petrogenesis of high-K granite from the Suffi Abad area, Sanandaj-Sirjan Zone, NW Iran. *Chemie*

Der Erde-Geochemistry, *71*, 363–376. https://doi.org/10.1016/j.chemer.2011.06.005

Azizi, H., Hadad, S., Stern, R. J., & Asahara, Y. (2019). Age, geochemistry, and emplacement of the ~40-Ma Baneh granite–appinite complex in a transpressional tectonic regime, Zagros suture zone, northwest Iran. *International Geology Review*, *61*, 195–223. https://doi.org/10.1080/00206814.2017.1422394

Azizi, H., Hadi, A., Asahara, Y., & Mohammad, Y. O. (2013). Geochemistry and geodynamics of the Mawat mafic complex in the Zagros Suture zone, northeast Iraq. *Central European Journal of Geosciences*, *5*, 523–537. https://doi.org/10.2478/s13533-012-0151-6

Azizi, H., & Jahangiri, A. (2008). Cretaceous subduction-related volcanism in the northern Sanandaj-Sirjan Zone. *Iran. Journal of Geodynamics*, *45*, 178–190. https://doi.org/10.1016/j.jog.2007.11.001

Azizi, H., Kazemi, T., & Asahara, Y. (2017). A-type granitoid in Hasansalaran complex, northwestern Iran: Evidence for extensional tectonic regime in northern Gondwana in the Late Paleozoic. *Journal of Geodynamics*, *108*, 56–72. https://doi.org/10.1016/j.jog.2017.05.003

Azizi, H., Lucci, F., Stern, R. J., Hasannejad, S., & Asahara, Y. (2018b). The Late Jurassic Panjeh submarine volcano in the northern Sanandaj-Sirjan Zone, northwest Iran: Mantle plume or active margin? *Lithos*, *308–309*, 364–380. https://doi.org/10.1016/j.lithos.2018.03.019

Azizi, H., Najari, M., Asahara, Y., Catlos, E. J., Shimizu, M., & Yamamoto, K. (2015). U-Pb zircon ages and geochemistry of Kangareh and Taghiabad mafic bodies in northern Sanandaj-Sirjan Zone, Iran: Evidence for intra-oceanic arc and back-arc tectonic regime in Late Jurassic. *Tectonophysics*, *660*, 47–64. https://doi.org/10.1016/j.tecto.2015.08.008

Azizi, H., Nouri, F., Stern, R. J., Azizi, M., Lucci, F., Asahara, Y., … Chung, S. L. (in press). New evidence for Jurassic continental rifting in the northern Sanandaj Sirjan Zone, western Iran: the Ghalaylan seamount, southwest Ghorveh. *International Geology Review*, 1–23. https://doi.org/10.1080/00206814.2018.1535913

Azizi, H., Zanjefili-Beiranvand, M., & Asahara, Y. (2015). Zircon U–Pb ages and petrogenesis of a tonalite–trondhjemite–granodiorite (TTG) complex in the northern Sanandaj-Sirjan zone, northwest Iran: Evidence for Late Jurassic arc–continent collision. *Lithos*, *216*, 178–195. https://doi.org/10.1016/j.lithos.2014.11.012

Badr, A., Davoudian, A. R., Shabanian, N., Azizi, H., Asahara, Y., Neubauer, F., … Yamamoto, K. (2018). A-and I-type metagranites from the North Shahrekord Metamorphic Complex, Iran: Evidence for Early Paleozoic post-collisional magmatism. *Lithos*, *300*, 86–104. https://doi.org/10.1016/j.lithos.2017.12.008

Baharifar, A., Moinevaziri, H., Bellon, H., & Piqué, A. (2004). The crystalline complexes of Hamadan (Sanandaj–Sirjan zone, western Iran): Metasedimentary Mesozoic sequences affected by Late Cretaceous tectono-metamorphic and plutonic events. *Comptes Rendus Geoscience*, *336*, 1443–1452. https://doi.org/10.1016/j.crte.2004.09.014

Bayati, M., Esmaeily, D., Maghdour-Mashhour, R., Li, X. H., & Stern, R. J. (2017). Geochemistry and petrogenesis of Kolah-Ghazi granitoids of Iran: Insights into the Jurassic Sanandaj-Sirjan magmatic arc. *Chemie Der Erde-Geochemistry*, *77*, 281–302. https://doi.org/10.1016/j.chemer.2017.02.003

Berberian, F., & Berberian, M. (1981). Tectono-plutonic episodes in Iran. Zagros Hindu Kush Himalaya Geodynamic Evolution (pp. 5–32). Geodynamic series, American Geophysics Union.

Cabanis, B., & Lecolle, M. (1989). Le diagramme La/10-Y/15-Nb/8: Un outil pour la discrimination des series volcaniques et la mise en evidence des processus de mélange et/ou de contamination crustale. *C.R. Acad. Sci. Serr. II*, *309*, 2023–2029.

Chiu, H. Y., Chung, S. L., Zarrinkoub, M. H., Mohammadi, S. S., Khatib, M. M., & Iizuka, Y. (2013). Zircon U–Pb age constraints from Iran on the magmatic evolution related to Neotethyan subduction and Zagros orogeny. *Lithos*, *162*, 70–87. https://doi.org/10.1016/j.lithos.2013.01.006

Chung, S. L., Wang, K. L., Crawford, A. J., Kamenetsky, V. S., Chen, C. H., Lan, C. Y., & Chen, C. H. (2001). High-Mg potassic rocks from Taiwan: implications for the genesis of orogenic potassic lavas. *Lithos*, *59*(4), 153–170.

Condie, K. C. (2005). High field strength element ratios in Archean basalts: A window to evolving sources of mantle plumes? *Lithos*, *79*, 491–504. https://doi.org/10.1016/j.lithos.2004.09.014

Deevsalar, R., Shinjo, R., Ghaderi, M., Murata, M., Hoskin, P. W. O., Oshiro, S., … Neill, I. (2017). Mesozoic-Cenozoic mafic magmatism in Sanandaj-Sirjan Zone, Zagros Orogen (Western Iran): Geochemical and isotopic inferences from Middle Jurassic and Late Eocene gabbros. *Lithos*, *284*, 588–607. https://doi.org/10.1016/j.lithos.2017.05.009

Esna-Ashari, A., Tiepolo, M., Valizadeh, M. V., Hassanzadeh, J., & Sepahi, A. A. (2012). Geochemistry and zircon U–Pb geochronology of Aligoodarz granitoid complex, Sanandaj-Sirjan Zone, Iran. *Journal of Asian Earth Sciences*, *43*, 11–22. https://doi.org/10.1016/j.jseaes.2011.09.001

Fazlnia, A., Moradian, A., Rezaei, K., Moazzen, M., & Alipour, S. (2007). Synchronous activity of anorthositic and S-type granitic magmas in Chah-Dozdan batholith, Neyriz, Iran: Evidence of zircon SHRIMP and monazite CHIME dating. *Journal of Sciences*, *Islamic Republic of Iran*, *18*, 221–237.

Fazlnia, A., Schenk, V., Appel, P., & Alizade, A. (2013). Petrology, geochemistry, and geochronology of the Chah-Bazargan gabbroic intrusions in the south Sanandaj-Sirjan zone, Neyriz, Iran. *International Journal of Earth Sciences*, *102*, 1403–1426. https://doi.org/10.1007/s00531-013-0884-6

Fazlnia, A., Schenk, V., van der Straaten, F., & Mirmohammadi, M. (2009). Petrology, geochemistry, and geochronology of trondhjemites from the Qori Complex, Neyriz, Iran. *Lithos*, *112*, 413–433. https://doi.org/10.1016/j.lithos.2009.03.047

Hunziker, D., Burg, J. P., Bouilhol, P., & Quadt, A. (2015). Jurassic rifting at the Eurasian Tethys margin: Geochemical and geochronological constraints from granitoids of North Makran, southeastern Iran. *Tectonics*, *34*, 571–593. https://doi.org/10.1002/2014TC003768

Jahn, B. M., Wu, F., Lo, C. H., & Tsai, C. H. (1999). Crustal–mantle interaction induced by deep subduction of the continental crust: Geochemical and Sr–Nd isotopic evidence from post-collisional mafic-ultramafic intrusions of the northern Dabie complex, central China. *Chemical Geology*, *157*, 119–146. https://doi.org/10.1016/S0009-2541(98)00197-1

Khalaji, A. A., Esmaeily, D., Valizadeh, M. V., & Rahimpour-Bonab, H. (2007). Petrology and geochemistry of the granitoid complex of Boroujerd, Sanandaj-Sirjan Zone, Western Iran. *Journal of Asian Earth Sciences*, *29*, 859–877. https://doi.org/10.1016/j.jseaes.2006.06.005

Lechmann, A., Burg, J. P., Ulmer, P., Mohammadi, A., Guillong, M., & Faridi, M. (2018). From Jurassic rifting to Cretaceous subduction in NW Iranian Azerbaijan: Geochronological and geochemical signals from granitoids. *Contributions to Mineralogy and Petrology*, *173*(12), 102. https://doi.org/10.1007/s00410-018-1532-8

Maanijou, M., Aliani, F., Miri, M., & Lentz, D. R. (2013). Geochemistry and petrology of igneous assemblage in the south of Qorveh area, west Iran. *Chemie Der Erde-Geochemistry*, *73*, 181–196. https://doi.org/10.1016/j.chemer.2013.04.001

Mahmoudi, S., Corfu, F., Masoudi, F., Mehrabi, B., & Mohajjel, M. (2011). U-Pb dating and emplacement history of granitoid plutons in the northern Sanandaj-Sirjan Zone, Iran. *Journal of Asian Earth Sciences*, *41*, 238–249. https://doi.org/10.1016/j.jseaes.2011.03.006

Masoudi, F., Yardley, B. W. D., & Cliff, R. A. (2002). Rb-Sr geochronology of pegmatites, plutonic rocks and a hornfels in the region south-west of Arak, Iran." (2002): 249–254. *Journal of Sciences*, *Islamic Republic of Iran*, *13*, 249–254.

Mazhari, S. A., Bea, F., Amini, S., Ghalamghash, J., Molina, J. F., Montero, P., … Williams, I. S. (2009). The Eocene bimodal Piranshahr massif of the Sanandaj-Sirjan Zone, NW Iran: A marker of the end of the collision in the Zagros orogen. *Journal of the Geological Society*, *166*, 53–69. https://doi.org/10.1144/0016-76492008-022

Middlemost, E. A. K. (1985). *Magmas and Magmatic Rocks* (p. 266). London, UK: Longman.

Mousivand, F., Rastad, E., Meffre, S., Peter, J. M., Solomon, M., & Zaw, K. (2011). U-Pb geochronology and Pb isotope characteristics of the Chahgaz volcanogenic massive sulfide deposit, southern Iran. *International Geology Review*, *53*, 1239–1262. https://doi.org/10.1080/00206811003783364

Nasr-Esfahani, A. K. (2012). Tectonic setting of metabasites of the Neo-Tethyan oceanic remains in Sanandaj-Sirjan structural zone, west of Isfahan, central Iran, Islam. *Azad University Mashhad Branch*, *4*, 75–84.

Nouri, F., Stern, R. J., & Azizi, H. (in press). The Jurassic tourmaline-garnet-beryl semigemstone province in the Sanandaj-Sirjan Zone, western Iran. *International Geology Review*, https://doi.org/10.1080/00206814.2018.1539927

Pearce, J. A. (2008). Geochemical fingerprinting of oceanic basalts with applications to ophiolite classification and the search for Archean oceanic crust. *Lithos*, *100*, 14–48. https://doi.org/10.1016/j.lithos.2007.06.016

Pearce, J. A., Harris, N. B., & Tindle, A. G. (1984). Trace element discrimination diagrams for the tectonic interpretation of granitic rocks. *Journal of Petrology*, *25*(4), 956–983. https://doi.org/10.1093/petrology/25.4.956

Rudnick, R. L., & Gao, S. (2004). Composition of the Continental Crust. In H. D. Holland, & K. K. Turekian (Eds.), *Treatise on Geochemistry* (pp. 1–64). Amsterdam: Elsevier; *3*.

Sepahi, A. A. (2008). Typology and petrogenesis of granitic rocks in the Sanandaj-Sirjan metamorphic belt, Iran: With emphasis on the Alvand plutonic complex. *Neues Jahrbuch Für Geologie Und Paläontologie-Abhandlungen*, *247*, 295–312. https://doi.org/10.1127/0077-7749/2008/0247-0295

Sepahi, A., Jafari, S., & Mani-Kashani, S. (2009). Low pressure migmatites from the Sanandaj-Sirjan Metamorphic Belt in the Hamedan region (Iran). *Geologica Carpathica*, *60*, 107–119. https://doi.org/10.2478/v10096-009-0007-2

Sepahi, A. A., Jafari, S. R., Osanai, Y., Shahbazi, H., & Moazzen, M. (in press). Age, petrologic significance and provenance analysis of the Hamedan low-pressure migmatites; Sanandaj-Sirjan Zone, west Iran. *International Geology Review*, 1–16. https://doi.org/10.1080/00206814.2018.1517392

Sepahi, A. A., Salami, S., Lentz, D., McFarlane, C., & Maanijou, M. (2018). Petrography, geochemistry, and U–Pb geochronology of pegmatites and aplites associated with the Alvand intrusive complex in the Hamedan region, Sanandaj-Sirjan zone, Zagros orogen (Iran). *International Journal of Earth Sciences*, *107*, 1059–1096. https://doi.org/10.1007/s00531-017-1515-4

Shafaii Moghadam, H., & Stern, R. J. (2015). Ophiolites of Iran: Keys to understanding the tectonic evolution of SW Asia: II) Mesozoic ophiolites. *Journal of Asian Earth Sciences*, *100*, 31–59. https://doi.org/10.1016/j.jseaes.2014.12.016

Shahbazi, H., Siebel, W., Pourmoafee, M., Ghorbani, M., Sepahi, A. A., Shang, C. K., & Abedini, M. V. (2010). Geochemistry and U–Pb zircon geochronology of the Alvand plutonic complex in Sanandaj-Sirjan Zone (Iran): New evidence for Jurassic magmatism. *Journal of Asian Earth Sciences*, *39*, 668–683. https://doi.org/10.1016/j.jseaes.2010.04.014

Shakerardakani, F., Neubauer, F., Masoudi, F., Mehrabi, B., Liu, X., Dong, Y., … Friedl, G. (2015). Panafrican basement and Mesozoic gabbro in the Zagros orogenic belt in the Dorud-Azna region (NW Iran): Laser-ablation ICP–MS zircon ages and geochemistry. *Tectonophysics*, *647*, 146–171. https://doi.org/10.1016/j.tecto.2015.02.020

Shand, S. J. (1943). *The Eruptive Rocks* (2nd ed.). New York, NY: John Wiley; 444.

Sheikholeslami, M. R. (2015). Deformations of Palaeozoic and Mesozoic rocks in southern Sirjan, Sanandaj-Sirjan Zone, Iran. *Journal of Asian Earth Sciences*, *106*, 130–149. https://doi.org/10.1016/j.jseaes.2015.03.007

Shervais, J. (1982). Ti-V plots and the petrogenesis of modern and ophiolitic lavas. *Earth Planetary Sciences Letters*, *59*, 101–118. https://doi.org/10.1016/0012-821X(82)90120-0

Stefano, T., Mariano, P., Stefano, V., Alessandro, I., Amerigo, C., Cinzia, B., … Stefano, M. (2018). Early Jurassic rifting of the Arabian passive continental margin of the Neo-Tethys. Field evidence from the Lurestan region of the Zagros fold-and-thrust belt, Iran. *Tectonics*, *37*(8), 2586–2607. https://doi.org/10.1029/2018TC005192

Stocklin, J. (1968). Structural history and tectonics of Iran: A review. *AAPG Bulletin*, *52*, 1229–1258.

Sun, S. S., & McDonough, W. S. (1989). Chemical and isotopic systematics of oceanic basalts: Implications for mantle composition and processes. *Geological Society, London, Special Publications*, *42*, 313–345. https://doi.org/10.1144/GSL.SP.1989.042.01.19

Tavakoli, N., Davoudian, A. R., Shabanian, N., Azizi, H., Neubauer, F., Asahara, Y., & Bernroider, M. (2019). Zircon U-Pb dating, mineralogy and geochemical characteristics of the gabbro and gabbro-diorite bodies, Boein-Miandasht, western Iran. *International Geology Review*, 1–19. https://doi.org/10.1080/00206814.2019.1583139

Valizadeh, M. V., & Cantagrel, J. M. (1975). Premieres données radiométriques (K–Ar et Rb –Sr) sur les micas du complexes magmatique du Mont Alvand, Pres Hamadan (Iran occidental). *Comptes Rendus Academie Des Sciences Paris. Serie D*, *281*, 1083–1086.

Yajam, S., Montero, P., Scarrow, J. H., Ghalamghash, J., Razavi, S. M. H., & Bea, F. (2015). The spatial and compositional evolution of the Late Jurassic Ghorveh-Dehgolan plutons of the Zagros Orogen, Iran. *Geologica Acta*, *1313*, 0025–0043. https://doi.org/10.1344/GeologicaActa 2015.13.1.2

Zhang, H., Chen, J., Yang, T., Hou, Z., & Aghazadeh, M. (2018). Jurassic granitoids in the northwestern Sanandaj-Sirjan zone: Evolving magmatism in response to the development of a Neo-Tethyan slab window. *Gondwana Research*, *62*, 269–286. https://doi.org/10.1016/j.gr.2018.01.012

SUPPORTING INFORMATION

Additional supporting information may be found online in the Supporting Information section at the end of the article.

How to cite this article: Azizi H, Stern RJ. Jurassic igneous rocks of the central Sanandaj–Sirjan zone (Iran) mark a propagating continental rift, not a magmatic arc. *Terra Nova*. 2019;31:415–423. https://doi.org/10.1111/ter.12404